

PHOTONIC CRYSTALS AS REAR-SIDE DIFFUSERS AND REFLECTORS FOR HIGH EFFICIENCY SILICON SOLAR CELLS

S. Janz, P. Voisin, D. Suwito, M. Peters, M. Hermle, S.W. Glunz
Fraunhofer Institute for Solar Energy Systems ISE, Heidenhofstr. 2, D-79110 Freiburg
Corresponding author: Stefan Janz, Tel.: +49-761-4588-5261, Fax.: +49-761-4588-9250,
E-mail: stefan.janz@ise.fraunhofer.de

ABSTRACT: The results in this publication show that it is possible to fabricate photonic crystals through spin-coating of nano spheres made of Polymethylmethacrylate (PMMA) or SiO_2 , a subsequent infiltration with $\text{Si}_x\text{C}_{1-y}$ using plasma enhanced chemical vapour deposition and optional burning out of the PMMA spheres. The structures are highly ordered and show enhanced reflectivity in the wavelength region of 1300 nm (600 nm spheres). An implementation of such structures into the process chain of high efficiency solar cells was done successfully. After passivating the solar cells rear side with $\text{Si}_x\text{C}_{1-x}$ and generating the photonic structure the rear metal contact was established with laser ablation and Al evaporation. Reflectivity measurements show reduced reflection for the solar cells with photonic structures and conductivity measurements proof that the rear contacting was successful.

Keywords: photonic crystals, high efficiency, silicon carbide

1 INTRODUCTION

Photon absorption and advanced optical confinement have always been essential preconditions to success in thin-film solar cell concepts. Especially the total reflection on the cell's rear side, besides front texture and anti reflection coating (ARC), was and still is the crucial point to exhaust the current potential [1]. As crystalline Si wafer solar cells become thinner and thinner the rear side also comes more and more into focus. Besides electrical issues like surface passivation and rear side contacting concepts the optical behaviour of this part of the cell's surface is nowadays one of the top subjects for R&D. The standard high-efficiency approach of a full area metal contact deposited on a dielectric passivation layers leads to very high, but also very specular, reflection for long wavelength light. Though for pushing the photon harvesting to its limits additional effort has to be made.

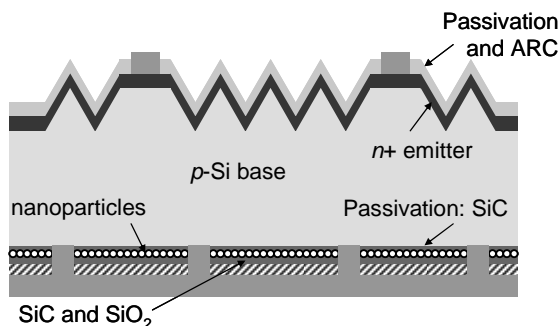


Figure 1: Sketch of the high efficiency solar cell structure with photonic crystals (PC) on the rear side.

This work wants to promote photonic crystals of $\text{Si}_y\text{C}_{1-y}$ as a material for improved photon management in high efficiency crystalline silicon solar cells (see Figure 1). It was already shown that the implementation photonic crystals on the rear-side of the thin film silicon solar cells can lead to significant current gain [1, 2]. In our approach, the implementation of a conductive $\text{Si}_x\text{C}_{1-x}:\text{H}$ passivation layer in combination with this highly doped photonic structure can address two crucial challenges of the solar cell's rear side and can be applied to c-Si surfaces with varying doping levels. At the same time this approach is highly flexible concerning the

contacting scheme and could possibly avoid complicated contacting procedures like local contacts. This would allow us to introduce a diffractive structure on the back side of a solar cell without the typical problems of surface recombination and difficult contacting. However, in a first step we applied local laser fired contacts to simplify the solar cell procedure and avoid additional challenges for the proof of concept.

2 EXPERIMENTAL AND RESULTS

2.1 Simulation

To estimate the effect of the photonic crystal on the absorption of the solar cell, we performed wave optical simulations to calculate the electromagnetic field inside the solar cell. For this calculation the RCWA (rigorous coupled wave analysis) method was used [3, 4]. The result of this calculation is on the one hand a rigorous description of the electromagnetic near field inside the cell and on the other hand a list of the diffracted directions and intensities for the light diffracted at the photonic crystal. Both information may be used to calculate the absorption of the solar cell and furthermore the absorption profile. The simulation method was used for a first optimization of the photonic crystal parameters. Parameters that were investigated are:

- the radius of the spheres, the photonic crystal consist of
- the material optimally used for the crystal
- whether the crystal itself or rather an inverted crystal should be used.

A complete discussion of the parameter optimization is beyond the scope of this work. As an example we show in Figure 2 a variation of the refractive index of the used spheres and its consequences on the absorption enhancement. It is important to note, that the calculated absorption enhancement is only a measure used for the optimization and underestimates the actual absorption enhancement as only the first reflection is calculated. Nevertheless Figure 2 shows that an optimum absorption enhancement is achieved for a photonic crystal with a period of ca. $\Lambda = 350$ nm (for solar cells with front side texture). The relative absorption enhancement increases fast with the refractive index of the used material. It is therefore convenient to use crystals with as high as

possible index materials. Currently, low index materials are typically used for reasons of availability, using high index matrix materials will however be one important future task.

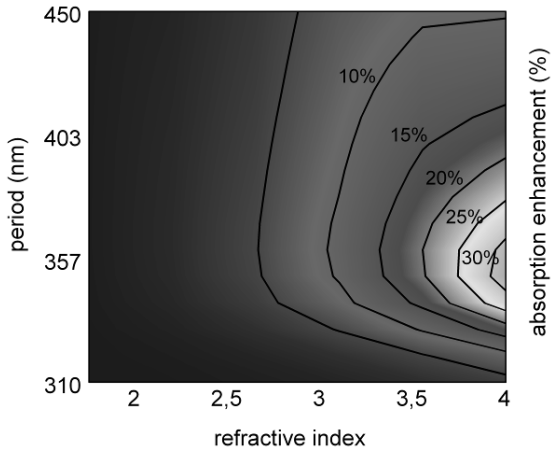


Figure 2: Dependency of the relative absorption enhancement on the photonic crystal period and its refractive index for a silicon solar cell without front side texture.

2.2 Deposition of the nano spheres

Two types of nano spheres were investigated in this study. The first ones are made of Polymethylmethacrylate (PMMA) and have a diameter of 380 nm and 600 nm. The second ones, produced by MicroParticles GmbH, are made of SiO_2 and have a diameter of 400 nm. Both types of particles are dissolved in a water solution.

In a first step the solutions with the 600 nm balls were simply dropped on one side of small glass samples ($30 \times 40 \text{ mm}^2$, 0.8 mm thickness) which came out of box and saw no additional cleaning before coating. This procedure leads to very inhomogeneous distributions of the nano spheres. However, the samples could be used for initial infiltration test to seek out the limits of infiltration.

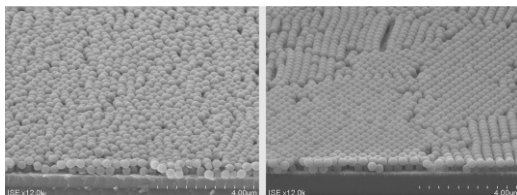


Figure 3: Scanning electron micrograph (SEM) of PMMA nano spheres spin coated on $\text{Si}_x\text{C}_{1-x}$ (left) with an over diluted solution and (right) with optimal dilution and spin coating parameters.

For the selective (only rear side) deposition of nano spheres on Si wafers we used the spin coating approach. After removal of the oxide on the back side of the wafer (hydrofluoric acid), a 70 nm thick layer of silicon rich, well-passivating silicon carbide ($\text{Si}_x\text{C}_{1-x}$) was deposited by PECVD (plasma enhanced chemical vapour deposition) on the rear side of the Si wafer. The precursor gases used in this process were SiH_4 , CH_4 and H_2 and low power densities were provided by a radio frequency (13.65 MHz) generator [5]. For the subsequent spin coating process, the surface tension energy of the

$\text{Si}_x\text{C}_{1-x}$ and the solutions containing the nano spheres are very important parameters in order to obtain a full and homogeneous coverage of the entire 4 inch wafer. It was found that no particular surface pre-treatment was necessary prior to the spinning of the nano balls. The only critical parameters are the hydrophilic properties of the solution and the adequate concentration of particles in it. Indeed, when not enough particles are present in the solution, they can be coated over the whole wafer but do not exhibit any order. This has for consequence that no diffraction effect can be observed. A Scanning Electron Micrograph (SEM) of such coating with PMMA nano spheres is presented in Figure 3 (left). The optimum dilutions and spinning conditions were found for both types of nano balls and SEM pictures of such coatings are presented in Figure 3 (right) for PMMA and in Figure 4 for the SiO_2 spheres. The micrographs make sure that we can obtain two homogeneous layers of PMMA nano particles, exhibiting a short distance order; and a monolayer of SiO_2 nano particles, which is not always fully closed, but still exhibits a short distance order. A simple observation with the eyes confirms after spin coating whether the nano spheres exhibit diffractive properties.

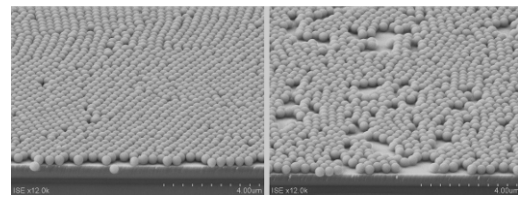


Figure 4: SEM of a monolayer of SiO_2 nano spheres deposited on $\text{Si}_x\text{C}_{1-x}$.

2.3 Inverted photonic structures

After spin coating of the nano spheres they were embedded in a $\text{Si}_y\text{C}_{1-y}$ matrix using PECVD. The same plasma reactor was used as for the $\text{Si}_x\text{C}_{1-x}$ passivation layer. In contrast to that process we applied the additional microwave plasma source (2.45 GHz) and diborane (B_2H_6) in order to dope the matrix material. The average power density during infiltration was adjusted to 20 mW/cm^2 to avoid sputtering of the PMMA spheres and to reduce growth rates. To enabling an infiltration of the space between substrate surface and spheres we applied low gas flows and low pressure ($<0.1 \text{ mbar}$).

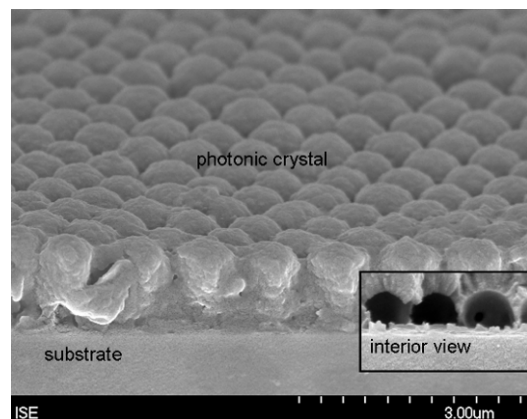


Figure 5: SEM of the $\text{Si}_y\text{C}_{1-y}$ photonic crystal structure on a glass substrate.

Subsequently the spheres were burned out at $>400^{\circ}\text{C}$ in a simple oven under ambient air. The evaporated PMMA spheres (see Figure 5) consist perfectly spherical and highly ordered hollows. In this example one can see that the average diameter of the photonic crystals (PC) is around 600 nm, which is in perfect accordance to the average PMMA spheres' radii. The adhesion behaviour of such layers was excellent on glass samples (for 600 nm spheres) but exhibited some problems on the Si wafer/ $\text{Si}_x\text{C}_{1-x}$ -passivation layer system (see chapter 2.4)

In Figure 6 the reflectance measured with a spectrophotometer *Carry 500i* scanning from 250 to 2500 nm wavelength before and after burning out of the PMMA spheres is showing the effect of inverting. The embedded spheres (600 nm) have a still weakly pronounced reflectance signal (light grey) at around 1400 nm. The burning out of the spheres (inverting) leads to a shift of the maximum to shorter wavelengths and an increase in signal (black). Although the effect of enhanced reflectance is still too wide in the infrared region for a silicon solar cell (bandgap of 1.1 eV) the enhanced scattering effect of the PC should in any case lead to an improved photon harvesting. However, we decided to focus on nano spheres with diameters of 380 nm for the solar cell approach.

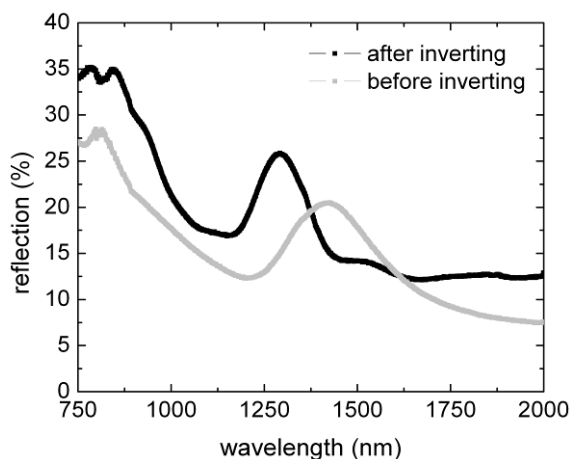


Figure 6: Reflectance measurements of the $\text{Si}_y\text{C}_{1-y}$ photonic structure (light grey) and after (black) burning out (inverting) of the PMMA spheres.

2.4 Solar cell fabrication

The starting material for the high efficiency solar cells were Float-Zone (FZ) [100], p-type, 0.5 Ωcm , shiny etched, 4 inch silicon wafers. The front sides were kept flat for some cells, while some others were textured with the highly effective inverted pyramids. The front side texture was first fabricated on the starting material with photolithography and a wet chemical etching in a KOH bath. The emitter was then diffused on the front side by a phosphorous diffusion performed at 790°C for 30 min. The resulting emitter exhibits a sheet resistance of 120 Ω/sq . A 105 nm thick thermal oxide was subsequently grown on both sides. This oxide was used on the one hand side as a passivation layer and on the other hand side as anti reflection coating (ARC) on the front side. After removal of the oxide on the back side, a 70 nm thick layer of silicon rich, well-passivating silicon carbide ($\text{Si}_x\text{C}_{1-x}$) was deposited by PECVD. After spin

coating of the PMMA and SiO_2 nano spheres with a diameter of 380 nm on these layers, they were infiltrated with the $\text{Si}_y\text{C}_{1-y}$ matrix material (see chapter 2.3) and covered by either 100 nm or 1 μm PECVD SiO_x . The SiO_x layers were applied to enable a smooth layer stack/metal interface and thereby prevent unwanted absorption effects. After this infiltration and deposition sequence, the PMMA spheres were burned out on a hot plate at $>400^{\circ}\text{C}$ for 12 min. Although foregoing test infiltrations on glass as well as on passivated Si substrates led to good adhesion, a peeling off of the layers took place on all the solar cell samples. These solar cells could not be further processed. First investigation led to the conclusion that the spin-coating and drying process seems to have significant influence on the infiltration behaviour of $\text{Si}_y\text{C}_{1-y}$. However, further optimisation will be needed for a reliable inverting process including the 380 nm PMMA nano spheres.

Continuing with samples containing SiO_2 nano spheres the back side contacts were performed by laser ablation of the rear stack system with a pitch of 800 μm . A 1030 nm wavelength laser with a pulse length of 1.5 μs was used. The varied process parameters are summarised in Table I.

Table I: Variations of the laser process parameters used to open the optical structure and the SiO_2 layer.

	SiO_2 thickness (μm)	Power (W)	Repetition
Wafer A	0.1	5.45	1 x
Wafer B	1	5.45	1 x
Wafer C	1	3.75	3 x

In Figure 7 SEM pictures of contact openings with the parameters from Wafer B and C are shown. One can see that the stack of infiltrated nano spheres and the covering 1 μm thick PECVD silicon dioxide can be successfully opened. Therefore, we expect that the same process on wafer A with a thinner SiO_x layer also leads to a sufficient opening of the structure. A 2 μm thick aluminium layer was then deposited by evaporation on the back side to establish the back contact of the solar cell.

Finally, the front side contacts were fabricated by opening the ARC, evaporating Ti-Pd-Ag, and a lift off process to produce the seed layer. Unfortunately the very last solar cell process, the thickening of the contacts with a standard silver electroplating process, could not be finished in time.

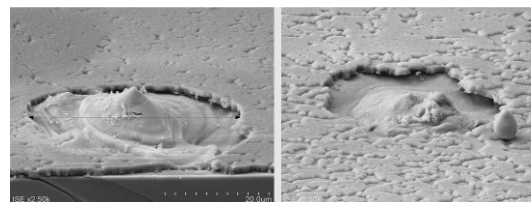


Figure 7: SEM pictures showing the back side contact opening with laser ablation, with a power of 5.45 W and 1 repetition (left) and a power reduced to 3.75 W and 3 times lasering on each contact (right).

However, reflectivity measurements of the solar cell samples could be made and are shown in Figure 8. The

reference samples (dotted lines) are solar cells with a similar front side and a 70 nm $\text{Si}_x\text{C}_{1-x}/1 \mu\text{m SiO}_x$ PECVD layer stack on the back side. In the wavelength region exceeding 1000 nm a clearly reduced reflection can be found for the samples with embedded nano spheres. Especially for the cells with no front texture this characteristic is significantly pronounced and points to an enhanced scattering effect on the solar cell's rear side. However, the reduced reflection can also be caused by other effects such as plasmon absorption at the SiO_x/Al interface and the final decision whether we were successful or not will have to wait for the quantum efficiency measurement of the solar cells.

Another encouraging result was the electrical measurement on some test samples which show no increase in series resistance and therefore proof the successful contact formation on the solar cell's back side.

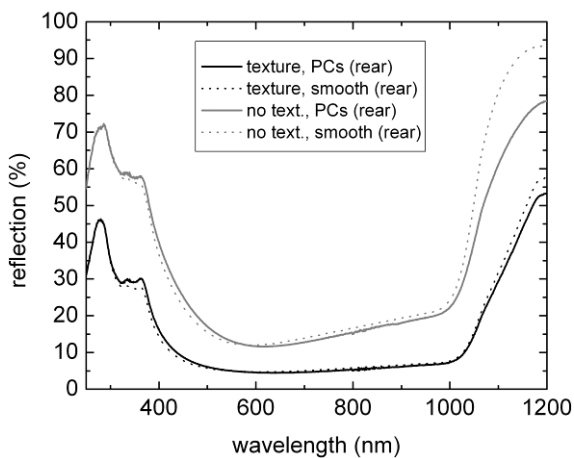


Figure 8: Reflection measurement over wavelength for different solar cell structures with textured front side (black) and/or photonic crystals on the rear side (solid).

3 SUMMARY AND CONCLUSIONS

In order to estimate the effect of the photonic crystals (PC) on the absorption of the Si high efficiency solar cell, we performed wave optical simulations using the RCWA (rigorous coupled wave analysis) method to calculate the electromagnetic field inside the solar cell. We could show that an optimum absorption enhancement is achieved for a photonic crystal with a period of ca. $\Lambda = 350$ nm. The relative absorption enhancement increases fast with the refractive index of the used matrix material. It is therefore convenient to use crystals with as high as possible index materials.

Two types of nano spheres, Polymethylmethacrylate (PMMA) and SiO_2 with diameters of 380 nm and 600 nm were investigated in this work. In a first step the water solutions with the 600 nm balls were simply dropped on small glass samples which led to very inhomogeneous distributions of the spheres. For the deposition of spheres on 4 inch Si wafers we used the spin coating approach. It was found that no particular surface pre-treatment was necessary prior to the spinning and that the hydrophilic properties of the solution and the adequate concentration of particles in it are of much more importance. We could obtain two homogeneous layers of PMMA nano particles, exhibiting a short distance order and a

monolayer of SiO_2 nano particles, which is not always fully closed, but still exhibits a short distance order. A simple observation with the eyes confirmed us after spin coating that the nano particles exhibited diffractive properties.

After spin coating of the silicone spheres they were embedded in a $\text{Si}_y\text{C}_{1-y}$ matrix using PECVD in the same reactor as for the passivation layer. Subsequently the spheres were burned. They consist perfectly spherical and highly ordered hollows (photonic crystals). The adhesion behaviour of such layers was excellent on glass samples and for the 600 nm spheres. The reflectance measurements before and after burning out of the PMMA spheres is definite proof of the effect of inverting.

On FZ, shiny etched, 4 inch silicon wafer PMMA and SiO_2 nano spheres with a diameter of 380 nm were spin coated on the $\text{Si}_x\text{C}_{1-x}$ passivation, infiltrated with the $\text{Si}_y\text{C}_{1-y}$ matrix material and covered by PECVD SiO_x . After this infiltration the PMMA spheres were burned out and a peeling off of the layers took place on all solar cell samples. Besides the influence of the spin-coating and drying process on the infiltration behaviour of $\text{Si}_y\text{C}_{1-y}$ the additional SiO_x layer could also be responsible for mechanical stress and enhanced delaminating of the photonic structures. On samples containing SiO_2 nano spheres the back side contacts were performed by laser ablation and evaporation of an aluminium layer. Electrical measurement on some test samples show no increase in series resistance and therefore proof the successful contact formation on the solar cells' back sides. Reflectivity measurements in the wavelength region exceeding 1000 nm show a reduced reflectance pointing to enhanced scattering when embedded nano spheres are involved. As the reduced reflection can also be caused by other effects such as plasmons absorption we still have to carry out quantum efficiency measurement of the solar cells to confirm the positive effect of the photonic structures.

The results in this publication show that it is possible to fabricate photonic crystals out of $\text{Si}_y\text{C}_{1-y}$ with PECVD. The structures are highly ordered and we are confident that they can be made electrically conductive with additional doping and therefore a simple rear side contact formation should not be out of scope.

4 ACKNOWLEDGEMENTS

The authors would like to thank S. Seitz, T. Leimenstoll, U. Jäger and F. Schätzle for process technology and C. Schetter as well as H. Steidl for keeping the plasma reactors running. The authors would also like to thank L. Steidl from University of Mainz for supplying us with PMMA beads.

This work was supported by the German Federal Ministry for the Environment, Nature Conservation and Nuclear Safety under contract number 0329849A (Th-ETA). M. Peters acknowledges the DFG project "Nanosun" (PAK 88) for financial support.

5 REFERENCES

- [1] Peter Bermel, Chiyan Luo, Lirong Zeng, Lionel C. Kimerling, and John D. Joannopoulos, "Improving thin-film crystalline silicon solar cell efficiencies

- with photonic crystals", *Optics Express*, Vol. 15, No. 25, (2007) p. 16986-17000.
- [2] P.G. O'Brien, N.P. Kherani, A. Chutinan, G.A. Ozin, S. John and S. Zukotinsky, "Silicon Photovoltaics Using Conducting Photonic Crystals Back-Reflectors", *Adv. Mater.* 2008, 20, p. 1577-1582.
- [3] M.G. Moharam, "Stable implementation of the rigorous coupled-wave analysis for surface relief gratings: enhanced transmittance matrix approach" *J. Opt. Soc. Am. A*, 12, 5 (1995)
- [4] Ph. Lalanne, M.P. Jurek, "Computation of the near-field pattern with the coupledwave method for transverse magnetic polarization", *J. Mod. Optics* 45, No. 7, 1357-1374 (1998).
- [5] D. Suwito, T. Roth, D. Pysch, L. Korte, A. Richter, S. Janz, S. W. Glunz, "Detailed study on the passivation mechanism of $a\text{-Si}_x\text{C}_{1-x}$ for the solar cell rear side", Proceedings of the 23rd EUPVSC, Valencia, Spain (2008) pp. 1023-1028.